INVESTIGATION OF ORTHOGONAL SPACE-TIME BLOCK CODES USING A MIMO HARDWARE DEMONSTRATOR

R. Seeger, L. Brötje, K.D. Kammeyer

Department of Communications Engineering
Universität Bremen
{seeger, broetje, kammeyer}@ant.uni-bremen.de

ABSTRACT

In this paper we present a multiple antenna system for industrial, scientific, and medical (ISM)-band transmission (MASI). The hardware demonstrator was developed and realized at our institute. It enables multiple input multiple output (MIMO)-communication applications and is capable to transmit arbitrary signals using 8 transmit and 8 receive antennas in parallel. It operates in the 2.4 GHz ISM-band. The hardware concept is introduced and some design specifications are discussed. As an application example, we will focus on one specific class of transmit diversity schemes: orthogonal space-time block codes (OSTBC). Channel estimation and carrier offset estimation are essential tasks in coherent receivers. However, they are also some kind of error sources due to the imperfectness of the employed algorithm. We will show by simulation and measurement results, that OSTBC based systems are more sensitive to channel estimation errors and/or carrier frequency offsets than conventional single transmit antenna systems. The consequence is that the diversity gain decreases significantly in the case of estimation errors.

Keywords: Hardware Demonstrator, MIMO, OSTBC, Alamouti

1. INTRODUCTION

One impetus to built a MIMO hardware demonstrator is that the assumptions made about real channels may be incorrect, and the behavior of MIMO systems should be investigated under realistic conditions. Therefore it is sufficient to transmit and receive over a real channel and process the received data offline at the workstation environment. This basic idea roots in [Haa99] where a single antenna system was realized at the University of Bremen. Furthermore, offline processing significantly reduces the complexity of the simulator. In contrast to a realtime simulator [GMea01], which is based on suboptimal frontend processing (due to strict timing constraints in connection with limited performance of DSP chips), this concept has enabled us to freely investigate optimal and suboptimal algorithm implementations. On the other hand, we do not claim to substitute a MIMO channel sounder. A channel sounder is a high accurate measurement system to precisely acquire the (MIMO) channel parameters. This requires extraordinary effort on e.g. calibrated and synchronized time bases at the transmitter and receiver, highly linear frontend amplifiers, and calibrated antenna arrays. In contrast, the objective of our demonstrator is to evaluate
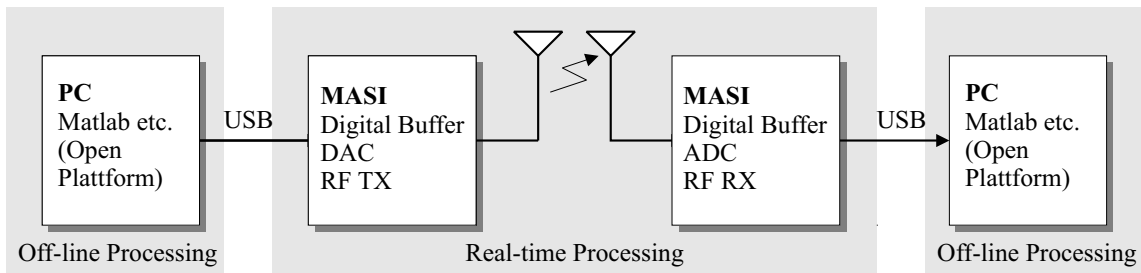
Fig. 1: Principle block diagram

MIMO algorithms under non-idealized environments deploying common hardware components. Moreover, thanks to selectable frontend processing we can handle arbitrary radio interface standards, such as single carrier, multicarrier and spread spectrum MIMO systems.

2. HARDWARE CONCEPT

2.1. Top-level System Description

The top-level system is diagrammed in Fig. 1. At the workstation environment in-phase and quadrature (I/Q) data, e.g. Hiperlan/2 or UMTS frames, are generated by the simulation system of choice. The impulse shaping is done in the digital domain. The data is scaled and quantized to meet the hardware demonstrator concerns and finally stored into a file. Due to its wide distribution the USB interface is chosen to connect the hardware demonstrator with the workstation. To transfer the I/Q data via the USB interface we use a customized application software which allows us to set several parameters, like sample rate (from external or internal clock), local oscillator (LO) frequency tuning value and assignment of data files to corresponding antennas. Furthermore, in a Matlab environment we can directly access the demonstrator by calling a Matlab function. This is useful for fully automated measurements. Inside the demonstrator the I/Q data is stored into digital buffers which are addressed in a circular manner: the increment pointers for memory accesses wrap to the beginning of the buffer when its end is reached. The currently addressed I/Q words are fed to a digital-to-analog converter (DAC), whose analog baseband output signals drive the radio frequency (RF) stage, which performs up-conversion to the desired RF frequency band.

At the receiver, the RF passband signal is down-converted to the complex baseband and undergoes analog-to-digital conversion. A snapshot is stored into a digital buffer. Because frame synchronization is not implemented in hardware the receive buffer has doubled length of the transmit buffer to ensure that at least one complete frame is captured. The sample rate is adjustable up to 80 MHz and may be chosen from a set of internally predefined frequencies or an external source. The request for extensibility of the hardware demonstrator led to a full modular architecture; for each antenna the connected transmitter or receiver hardware has its own plug-in module (see Fig. 2). The digital clock and LO signal is provided to all modules by a central clock base to ensure inter module synchronization of sample rate and carrier phase.

Low cost software radios are the main driver for modern radio architectures (universal receivers that can accommodate many different standards). Consequently, this type of receiver gain increased attention. An all digital receiver performs all its operations in the digital domain, except the frontend baseband
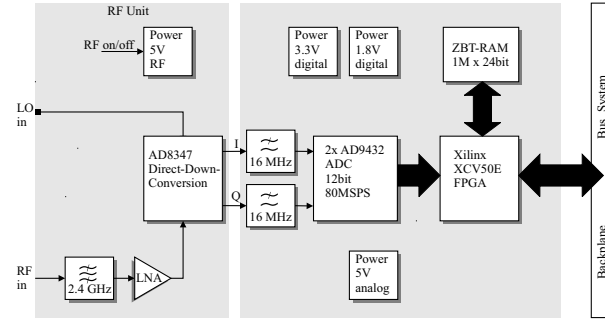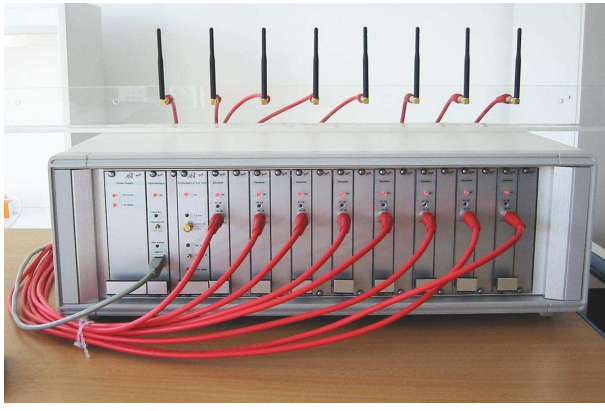
Fig. 2: The Multiple Antenna Receiver for ISM-Band Transmission. Currently, the receiver and transmitter are equipped with 8 modules. Block diagram of one receiver module

translation and anti-aliasing filtering. Its ADC sampling clock is not synchronized to the transmitter symbol clock. Therefore, many analog components, such as the voltage-controlled-oscillator (VCO), are not required. Thus, it can be smaller, more robust, and less expensive. However, as a fixed sampling clock is used which is not synchronized to the transmitter clock, symbol timing and carrier recovery have to be accomplished in the digital domain. In order to reduce analog component count in the RF stage the direct conversion (or homodyne) architecture is implemented, which performs passband to baseband translation and vice versa directly without IF stages. Traditionally the direct conversion architecture was considered impractical due to severe realization problems. So far, it was hardly possible to fulfill all requirements like exceptionally linear LNA and mixer circuits, as well as the LO isolation resulting in a lower sensitivity compared to heterodyne receivers [Lee98]. However, recent advances in chip technology enabled robust direct conversion frontends.

3. AN APPLICATION EXAMPLE:ORTHOGONAL SPACE-TIME BLOCK CODES

Often transmit diversity techniques are investigated in highly idealized simulation environments. In the following we will discuss the so called orthogonal space-time block codes (OSTBC) under more realistic conditions. Channel estimation and carrier offset estimation are essential tasks in coherent receivers. However, they are also some kind of error sources due to the imperfectness of the employed algorithm.

Alamouti [Ala98] discovered a remarkable transmit diversity scheme for transmission with two antennas. This scheme supports maximum-likelihood detection based only on linear processing at the receiver and is able to achieve full diversity provided by the number of transmit and receive antennas. The input symbols to the ST block encoder are divided into groups of two symbols each $\{s_1, s_2\}$. At a given symbol period, s_1 and $-s_2^*$ are transmitted from antenna 1 and 2, respectively, and at the consecutive symbol period, s_2 and s_1^* are transmitted from antenna 1 and 2, respectively. Let h_1 and h_2 be the channel coefficients from the first and second transmit antennas, respectively. It is assumed that h_1 and h_2 are constant over two consecutive symbol periods. Consider a receiver with one receiver antenna and denote the received signals over two consecutive symbol periods as r_1 and r_2. Defining the code symbol vector $\mathbf{s} = [s_1 s_2]^T$ and the received vector $\mathbf{r} = [r_1 r_2^*]^T$, we get

$$\mathbf{r} = \mathbf{Hs} + \boldsymbol{\eta} \tag{1}$$

where the channel matrix

$$\mathbf{H} = \begin{bmatrix} h_1 & -h_2 \\ h_2^* & h_1^* \end{bmatrix},$$ (2)

and the noise vector $\boldsymbol{\eta} = [\eta_1 \eta_2^*]^T$ are used. The AWGN is represented by η_1 and η_2 which are modelled as i.i.d complex Gaussian random variables with zero mean and power spectral density $N_0/2$ per dimension. Hence $\boldsymbol{\eta}$ is a Gaussian random vector with zero mean and covariance $N_0 \mathbf{I}$.

The decoding procedure consists of a simple multiplication with the hermitian channel matrix $\hat{\mathbf{H}}^H$, hence

$$\hat{\mathbf{s}} = \hat{\mathbf{H}}^H \mathbf{H} \mathbf{s} + \hat{\mathbf{H}}^H \boldsymbol{\eta}$$ (3)

where $\hat{\mathbf{H}}$ is the *estimated* channel matrix. Considering imperfect channel estimation with an estimation error [SBF01]

$$\Delta h = \Delta h_{\text{noise}} + \Delta h_{\text{Doppler}}$$ (4)

it follows

$$\hat{\mathbf{H}} = \begin{bmatrix} h_1 + \Delta h_1 & -(h_2 + \Delta h_2) \\ h_2^* + \Delta h_2^* & h_1^* + \Delta h_1^* \end{bmatrix}.$$ (5)

The (soft) decoded symbol-vector $\hat{\mathbf{s}} = [\hat{s}_1 \hat{s}_2]^T$ can be obtained using (3) and (5)

$$\hat{\mathbf{s}} = \underbrace{\begin{bmatrix} |h_1|^2 + |h_2|^2 & 0 \\ 0 & |h_1|^2 + |h_2|^2 \end{bmatrix} \mathbf{s}}_{\text{desired}}$$ (6)

$$+ \underbrace{\begin{bmatrix} h_1 \Delta h_1^* + h_2^* \Delta h_2 & -h_2 \Delta h_1^* + h_1^* \Delta h_2 \\ -h_1 \Delta h_2^* + h_2^* \Delta h_1 & h_2 \Delta h_2^* + h_1^* \Delta h_1 \end{bmatrix} \mathbf{s}}_{\text{influence of estimation errors}}$$

$$+ \underbrace{\hat{\mathbf{H}}^H \boldsymbol{\eta}}_{\text{noise}}$$

From (6) it is clear that channel estimation errors lead to spatial intersymbol interference (ISI) if the estimated channel matrix $\hat{\mathbf{H}}$ is not unitary. (5).

Another major task for coherent receivers is the carrier frequency offset estimation and correction. Consider two consecutive received symbols r_1 and r_2. The frequency offset can be modelled by the time-domain multiplication with the two phasors $e^{j\varphi_1}$ and $e^{j\varphi_2}$, respectively. Of course, φ_2 can be expressed by $\varphi_2 = \varphi_1 + \Delta\varphi$, with $\Delta\varphi$ being the phase deviation between the phase error at time of r_1 and the phase error at time of r_2, so that $\Delta\varphi$ is proportional to the frequency deviation, if the phase errors results out of a CFO. Using the system model (1) it can be stated

$$\begin{bmatrix} e^{j\varphi_1} & 0 \\ 0 & e^{-j\varphi_2} \end{bmatrix} \begin{bmatrix} r_1 \\ r_2^* \end{bmatrix} = \begin{bmatrix} e^{j\varphi_1} & 0 \\ 0 & e^{-j\varphi_2} \end{bmatrix} (\mathbf{H}\mathbf{s} + \boldsymbol{\eta}).$$ (7)

Assuming perfect channel estimation conditions, i. e. $\hat{\mathbf{H}} = \mathbf{H}$, and neglecting the noise term in (7), we obtain

$$\begin{bmatrix} h_1^* & h_2 \\ -h_2^* & h_1 \end{bmatrix} \begin{bmatrix} e^{j\varphi_1} & 0 \\ 0 & e^{-j\varphi_2} \end{bmatrix} \begin{bmatrix} h_1 & -h_2 \\ h_2^* & h_1^* \end{bmatrix} \mathbf{s}$$

$$= \begin{bmatrix} |h_1|^2 e^{j\varphi_1} + |h_2|^2 e^{-j\varphi_2} & -h_1^* h_2 e^{j\varphi_1} + h_2 h_1^* e^{-j\varphi_2} \\ -h_2^* h_1 e^{j\varphi_1} + h_1 h_2^* e^{-j\varphi_2} & |h_2|^2 e^{j\varphi_1} + |h_1|^2 e^{-j\varphi_2} \end{bmatrix} \mathbf{s}. \qquad (8)$$

In contrast to a single transmit antenna system, the loss of orthogonality due to a (residual) frequency offset leads to *magnitude* variations. To verify these results, we did some indoor measurements in the 2.4 GHz ISM band at the University of Bremen, using the multiple antenna system. A burst of 1024 QPSK modulated data symbols was sent. The comparison of one simulated and three measured signal constellations with channel estimation and frequency offset is depicted by Fig. 3. In addition, symbol error rate simulations were conducted (see Fig. 4). Each frame consisted of 1024 data symbols and a preamble of 256 pilot symbols. The phase change from symbol to symbol was fixed to $\Delta\varphi = 2\pi\Delta fT = 0.0001$, where Δf and T denotes the carrier frequency offset and the symbol duration, respectively. The transmit power was normalized to 1. In case of the 64-QAM OSTBC transmission scheme the increased symbol error rate due to CFO is evidently. At a symbol error rate of 0.01 there is nearly no diversity gain available, furthermore, the performance of the OSTBC scheme can be worse than the conventional scheme with 1 transmit antenna for higher signal-to-noise ratios. It can be concluded, that the simulation results confirm the sensitivity of OSTBC based systems against phase errors.
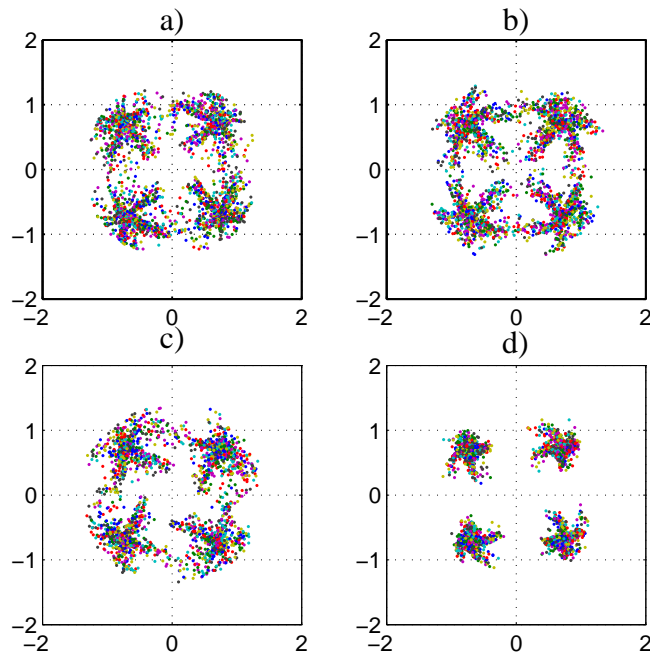
Fig. 3: Signal constellation diagrams for QPSK at the OSTBC decoder output with carrier frequency offset: a) simulated, b) - d) measured

4. CONCLUSIONS

In this paper we introduced a very flexibly low cost measurement system which allows the testing of nearly all MIMO communications setups currently under discussion. Arbitrary signals can be generated and transmitted in real time. However, the offline concept significantly reduces the complexity of the demonstrator.
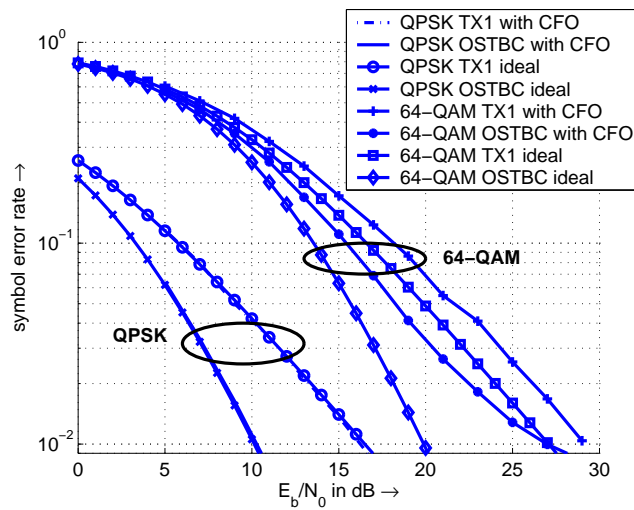
Fig. 4: Simulated symbol error curves (64 QAM, independent Rayleigh fading): The 1 transmit antenna scheme exhibits nearly the same performance with and without carrier frequency offset (CFO), whereas the OSTBC scheme shows a strong increased symbol error rate in the case of CFO. The transmit power was normalized to 1.

As an application example, the influences of carrier frequency offsets, or, more general, phase errors including phase jitter and phase noise, on a system with transmit diversity scheme according to Alamouti were discussed. Signal constellation diagrams illustrates the effects of carrier frequency offsets. Additionally, measurements in the 2.4 GHz ISM band verify the theoretical results. The mathematical formulation reveals, that the orthogonality of the OSTB coding scheme is lost, which makes it more sensitive to phase errors compared to a single transmit antenna system. This was also shown by means of symbol error rate simulations.

5. REFERENCES

[Ala98]   S.M. Alamouti. A simple transmit diversity technique for wireless communications. *IEEE Journal on Selectes Areas in Commununications*, 16(8):1451–1458, October 1998.

[GMea01] R. Gozali, R. Mostafa, and R.C. Palat et al. Virginia-Tech Space-Time Advanced Radio (VT-STAR). In *Proceedings of the IEEE Radio and Wireless Conference (RAWCON)*, page 227231, 2001.

[Haa99]   T. Haase. Aufbau einer digitalen Funkübertragungsstrecke bei 2.4 GHz für Anwendungen innerhalb von Gebäuden. Diplomarbeit (in German), Bremen, Germany, 1999.

[Lee98]   Thomas H. Lee. *The Design of CMOS Radio-Frequency Integrated Circuits*. Cambridge University Press, 1998.

[SBF01]   M. Stege, M. Bronzel, and Fettweis. On the Performance of Space-Time-Codes. In *VTC-Spring 2001*, Rhodos, 2001.